Edge-state Transport in Circular Quantum Point Contact Quantum Piezotronic Transistors

Yuankai Zhou, Yuncheng Jiang, Minjiang Dan, Gongwei Hu, Lijie Li, Yan Zhang

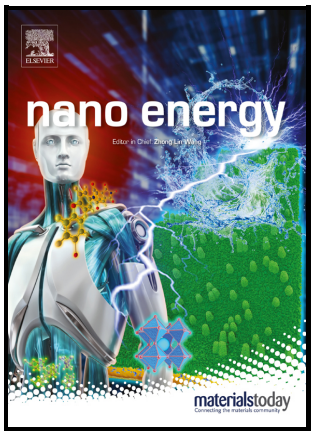

PII: S2211-2855(21)00260-3

DOI: https://doi.org/10.1016/j.nanoen.2021.106002

Reference: NANOEN106002

To appear in: *Nano Energy*

Received date: 10 January 2021
Revised date: 3 March 2021
Accepted date: 15 March 2021

Please cite this article as: Yuankai Zhou, Yuncheng Jiang, Minjiang Dan, Gongwei Hu, Lijie Li and Yan Zhang, Edge-state Transport in Circular Quantum Point Contact Quantum Piezotronic Transistors, *Nano Energy,* (2021) doi:https://doi.org/10.1016/j.nanoen.2021.106002

Edge-state Transport in Circular Quantum Point Contact Quantum Piezotronic Transistors

Yuankai Zhou[1, †], Yuncheng Jiang[1, †], Minjiang Dan[1, †], Gongwei Hu[1], Lijie Li[2] and Yan Zhang[1,3, *]

[1] *School of Physics, University of Electronic Science and Technology of China, Chengdu 610054, China*

[2] *Multidisciplinary Nanotechnology Centre, College of Engineering, Swansea University, Swansea, SA1 8EN, UK*

[3] *Beijing Institute of Nanoenergy and Nanosystems, Chinese Academy of Sciences; National Center for Nanoscience and Technology (NCNST), Beijing 100083, China*

† Those authors contribute equally to this work

[*]To whom correspondence should be addressed, E-mail: zhangyan@uestc.edu.cn

Abstract

Quantum piezotronic transistor is studied based on HgTe/CdTe topological insulator with a circular quantum point contact. The radius of the circular region is modulated by strain-induced piezoelectric potential. The electronic transport behavior of the edge and bulk states is explored by calculating the conductance and electronic density distribution under different Fermi energies and strains. Transport property of edge states is studied by machine learning method and the transport conductance can be effectively predicted. These results show that the neural network can be used for obtaining electronic transport properties, and it has great potential for optimizing and designing high-performance quantum piezotronic devices.

Keywords: Topological insulator, machine learning, quantum piezotronic devices, edge states

1. Introduction

Piezotronic and piezo-phototronic devices convert externally mechanical signals into electrical signals, which are good candidates for highly integrated silicon-based electronic devices [1]. Piezoelectric semiconductor materials such as ZnO, GaN, InN and CdS simultaneously have piezoelectric and semiconductor property [1], producing unprecedented characteristics and playing an important role in the development of nanogenerators [2], high-performance strain sensors [3-5], strain-gated field effect transistor [6, 7] and LEDs [8]. Many high-performance piezoelectric devices have been developed based on piezoelectric semiconductors, such as piezoelectric field effect transistor [9], solar cell [10], LED [11] and photon detector [12], which are high sensitivity and easy to regulate. The application of piezoelectric effect in emerging quantum materials such as two-dimensional materials and topological insulators has received extensive attention. Recently, the HgTe quantum well with an inverted band structure which could exhibit quantum spin Hall insulator state was predicted by Bernevig *et al.* [13] and experimentally confirmed by König *et al*. [14].

Topological insulators have received wide attention in quantum computing and high-temperature superconductor due to its unique metallic surface states and insulating bulk states. Electronic transport of edge states is ultralow power consumption and has ultrahigh device stability [15]. Previous studies have shown that externally applied electric field can drive topological phase transition from normal insulator to topological insulator [16, 17]. The required electric field is much strong [18] with the order of 10 MV/cm. Gate voltage provides ~100 kV/cm in experiments. Piezoelectric field can reach up to 10 MV/cm [19-21]. Strain can increase the bulk band gap of topological insulators [17, 22], making it possible for high temperature topological insulators [23]. The helical edge states of topological insulator are protected by time reversion symmetry [13, 14], giving rise to the robust property against the disorder regime and material structure [24, 25]. Furthermore, the superconductivity of edge

states can be observed by using the superconducting quantum interference for two-dimensional topological insulators [26]. Recently, high sensitivity strain sensor and quantum memory device based on topological insulators have been proposed [3, 4, 19, 27].

In this paper, we theoretically study the transport properties of edge states and bulk states for HgTe/CdTe quantum well topological insulator with a circular quantum point contact (QPC). The quantum point contact is formed between the circular region and both sides of the quantum well to modulate the electronic transport of topological insulator. The radius of the circular region is controlled by strain-induced piezoelectric potential. By calculating the conductance and electronic density distribution (EDD) under different Fermi energies and radiuses of circular quantum point contact, the electronic transport behaviors of the edge and bulk states are explored. We further employ machine learning to investigate the tuning of edge-state transports by externally applied strain. By training an artificial neural network with EDD, this network can effectively predict their conductance.

2. Electronic transport in quantum piezotronic devices with a circular quantum point contact

Figure 1 illustrates the topological insulator based on HgTe/CdTe quantum well. A thin HgTe layer is sandwiched between two CdTe layers, and a circular depletion region appears in the center of the system. This depletion region is created by the piezoelectric potential on the top of quantum wells. The constriction between the depletion region and boundaries of HgTe layer acts as the quantum point contacts [16]. Such topological quantum point contact structure has been realized experimentally based on HgTe quantum well [28]. Tuning the radius of depletion region is an effective way to control the width of quantum point contact. Applying a piezoelectric potential on the top of the quantum well, the extension of the depletion region is free to broaden or shrink. Figure 1(a) shows a large circular depletion region formed by the high piezoelectric potential. In the QPCs on both sides, band structure of the electrons is insulating with a finite gap [seeing left of Figure 1(a)]. In this case, edge-state

channels close and the electrons are blocked and reflected back, causing the "OFF" state of the system. The radius of the depletion region shrinks while the piezoelectric potential decreases. Figure 1(b) shows electronic transport when the radius of the circular insulation region is small (the QPCs are wide). This case corresponds to gapless band structure and the edge-state electrons can flow through the QPC without blocking, leading to the "ON" state.

The electronic transport properties such as the conductance, transmission and EDD in the quantum well are determined by the Schrödinger equation

$$H\psi = E\psi \quad (1)$$

where ψ is a wave function of electrons, E is an energy eigenvalue and *H* is a Hamiltonian. The transport properties can be obtained by solving the equation under specific boundary conditions. There are some typical boundary conditions in quantum systems such as Dirichlet, Neumann boundary conditions [29], and periodic boundary condition [30]. Dirichlet boundary condition is employed by setting a vanishing wave function at the boundary $\psi\big|_{\text{boundary}} = 0$ for the QPC structure [31].

In case of HgTe/CdTe quantum well topological insulator, the electronic properties are described by the four-band Hamiltonian [13]

$$H = \begin{pmatrix} \varepsilon_k + M_k & Ak_- & 0 & 0 \\ Ak_+ & \varepsilon_k - M_k & 0 & 0 \\ 0 & 0 & \varepsilon_k + M_k & -Ak_+ \\ 0 & 0 & -Ak_- & \varepsilon_k - M_k \end{pmatrix} \quad (2)$$

where $\varepsilon_k = C + V(x) - Dk^2$, $M_k = M - Bk^2$ with $k_\pm = k_x \pm ik_y$, $k^2 = k_x{}^2 \pm k_y{}^2$ and the relevant parameters are *A* = 364.5 meV nm, *B* = -686 meV nm^2, C = 0, D = -512 meV nm^2, and M = -10 meV [13].

According to previous studies, when the thickness of the quantum well is smaller than the critical value of 6.3 nm, the quantum well exhibits extremely weak conductance, indicating the normal insulator [32]. While the thickness is larger than 6.3 nm, gapless edge states appear and the quantum well maintains topological insulator [14]. In this study, we choose the thickness of 7 nm to ensure the existence of edge states.

When the electrons travel through the system, transport conductance can be given from Landauer-Büttiker formula [33, 34]

$$G = G_0 \sum_{m,n} |t_{mn}|^2 \quad (3)$$

where G_0 is the conductance unit of $2e^2/h$ and t_{mn} is the transmission coefficient for electrons injected from m-th input channel and scattering to the n-th output channel.

We use the tight-binding package KWANT to calculate the transmission properties of electrons in HgTe/CdTe quantum wells. KWANT is a user-friendly and high-efficient Python package for numerical quantum transport computation [29]. By applying the stable wave function algorithm to the wave function calculation, KWANT is superior to the commonly used Recursive Green Algorithm (RGF). We construct a Hall bar transport system with a circular quantum dot. Specifically, the width of transport system is fixed at W = 200 nm, and lattice constant is a = 1 nm. The length of the scattering region is L = 300 nm, and the radius R of the depletion region is in the range of 0 to 100 nm. Each site in the system is related by lattice translations. The onsite energy for each cubic lattice and hopping energy for two neighboring cubic are calculated by discretizing the **kp** Hamiltonian (2). By injecting electrons from the lead on one side, the conductance and the electronic distribution in the system can be obtained by KWANT. In our case, the transport conductance and wave functions in HgTe/CdTe topological insulator are calculated by KWANT. There are some tight-binding packages to calculate quantum transport, such as SMEAGOL and SIESTA [35-37].

For a small uniform strain *S* applied on the piezoelectric materials, the piezoelectric charges can be calculated by the polarization vector *P* which is given by [38] $(p)_i = (e)_{ijk}(S)_{jk}$, where e_{ijk} is the third-order piezoelectric tensor. According to constituting equation which can be given by piezoelectric theory [39, 40], piezoelectric potential induced by the piezoelectric charges inside a bulk material can be given by

$$V_{piezo} = \frac{PL_{piezo}}{\varepsilon_r \varepsilon_0} \quad (4)$$

where *P* is the polarization vector. L_{piezo} is the length of the piezoelectric material, ε_r and ε_0 are the relative dielectric constant and vacuum dielectric constant.

For zinc-blende structure material with shear strain s_{23}, the piezoelectric potential can be obtained as [41] $V_{piezo} = e_{14} s_{23} L / (\varepsilon_r \varepsilon_0)$, where e_{14} is piezoelectric coefficient, ε_r and ε_0 are relative and vacuum permittivity, L is material length. The radius of the depletion region can be given by $R = \alpha V_{piezo}$ and $\alpha = 225$ nm V^{-1} [42]. The piezoelectric material chooses CdTe, and its relevant material parameters are $e_{14} = 0.035$ C/m^2, $\varepsilon_r = 9.8$, and $L = 300$ nm.

3. Results and discussions

3.1. Piezotronic effect on edge-state transport

Figure 2 (a) shows the conductance at different Fermi energies as a function of strain. The conductance exhibits a distinct switching behavior. The conductance of $G_0 \left(= 2e^2 / h\right)$ corresponds to the "ON" state of device, and the zero conductance is the "OFF" state. All of the five Fermi energies are in the bulk gap of gapless band structure, and thus all of them are edge-state transport. When the Fermi energy is set at -8 meV which is close to the valence

band, there is a sharp transition from the "ON" state to the "OFF" state at R = 85 nm (s_{23} = 0.31%), indicating a quick switching behavior. As the Fermi energy increases and approaches to the conduction band, the R region with the "ON" conductance decreases. For E_F = 5 meV, there is a smooth transition between the "ON" and "OFF" state, meaning that the electrons travel partially through the QPC. When the Fermi energy is set at 1 meV, the conductance is significantly decreased at $s_{23} = 0.2\%$. There is the quantum interference between the transmitted and reflected electrons in the circular QPC. This interference effect forms the Fabry-Perot modes localized within the narrow QPC, giving rise to a partially transmitted conductance [31].

To illustrate it more clearly, Figures 2(b-d) show the EDDs of edge states under the radius of 20 nm (s_{23} = 0.07%), 35 nm (s_{23} = 0.13%) and 80 nm (s_{23} = 0.29%), respectively. The Fermi energy is fixed at 5 meV. In case of a small depletion region radius R = 20 nm, the width of QPC in both sides of the system is large and the electrons can freely pass through the QPC almost without blocking, leading to the conductance $2G_0$, as shown in Figure 2(b). When the radius is R = 35 nm in Figure 2(c), the electrons partially travel through the system and the other is reflected back along the upper boundary, meaning the conductance $0 < G < G_0$ [43]. While the electrons are completely blocked and the conductance is zero at R = 80 nm in Figure 2(d).

3.2.Piezotronic effect on bulk-state transport

Figure 3 shows the bulk-state conductance as a function of strain for different Fermi energies from 17 meV to 29 meV. In terms of conductance plateau, one obvious distinction between edge-state and bulk-state transport in topological insulators is their number of the plateau. Edge states contribute one plateau, and bulk states have many channels. For instance, Figure 3 shows that with the increase of Fermi energy, the number of bulk channels increases, and hence the maximum of conductance plateau grows.

Figure 4 shows the EDDs at different strains. The Fermi energy is set at 30 meV and four conductance channels appear. When those four bulk states are injected from the left lead, they exhibit different transport properties. When the radius of the depletion region is as large as 80 nm (s_{23} = 0.29%), all electrons are blocked and the conductance is close to 0, as shown in Figure 4(a). As the radius decreases, the QPCs on the upper and lower boundary become wide. In this case, there are three partially opening channels and one closing channel in Figure 4(b) at R = 50 nm. Figure 4(c) shows that in R = 25 nm all channels are open but the electrons only partially pass and the other part is reflected back to the lead. When the radius is reduced to much small such as R = 10 nm in Figure 4(d), the electrons travel through the system almost unblocked, as shown in Figure 4(d).

3.3. Machine learning method for edge-state transport

The machine learning (ML) is very important for search, discovery, and optimization of material science and technology in the future (see Table 1 for a summary of related work on ML in materials science and technology). ML algorithms can achieve the equivalent functions for identifying topological phase transitions [44-46]. ML algorithm has very higher efficiency and accuracy than traditional algorithms[47, 48]. The powerful information processing capabilities of ML algorithms can help break physical limits, for example, recognizing and imaging subwavelength features from the far field [49]. Even ML algorithms can be used to explore new physics, such as discovering new materials [50], predicting materials properties [51], and obtaining the experimental conditions for materials. [52].

Dense Convolutional Network (DenseNet) is a typical artificial neural network algorithm of machine learning [53]. DenseNet is used for image processing, which can achieve high performance with a small number of parameters.

In this study, The EDD matrix reflects the spatial density distribution features of electrons, which can be regarded as image data. DenseNet can be used to establish the correspondence between these features and conductance. The conductance is obtained from

image data of electron density distribution matrix processed by DenseNet. Figure 5(a) shows the structure of DenseNet for the conductance calculations, which includes three layers: the input layer, the hidden layer, and output layer. The hidden layer includes 4 convolutional layers, 3 pooling layers, 4 dense blocks, a global pooling layer, and a fully connected layer. There are 382,942 parameters in the network. The input images are 201 pixels by 299 pixels, the input layer has 60099 input nodes. The output layer is a neuron for regressing conductance. The EDD matrix is input data. In our calculation, four dense blocks are used to extract the EDD features in the hidden layer. DenseNet can predict unknown data by learning existing knowledge, and has great generalization ability. 1782 EDD matrices are used for the training process. The trained DenseNet was used to predict the 100 EDD matrices (E_F = -5 meV) that were not added to the training set, R-squared is 0.999 of the conductance from KWANT and machine learning.

GaN and ZnO have attracted enormous research interests due to their unique properties. In theory, InN/GaN quantum well can form topological insulator based on the intrinsic polarization [54]. ZnO/CdO quantum well can form topological insulator under stress and be used as quantum piezotronic devices [55]. In experiment, μ-LED applications can be designed based on InGaN/GaN multiple quantum well [56]. Nanostructures including ZnO have excellent performance in photodetectors [57], adaptive electronics and optoelectronics such as pressure imaging, LED, luminescence [58]. Figure 5(b) shows the edge-state conductance of the calculation by KWANT and machine learning prediction of some popular relevant materials such as GaN and ZnO. The transition points of “ON” and “OFF” state are 0.008%, 0.018%, 0.31% for ZnO, GaN, CdTe, respectively. The machine learning prediction shows a good agreement for three materials.

Figure 5(c) shows that the training loss function curve gradually decreases and converges near 0 after training for about 50 epochs, which proves that DenseNet has learned and established the relationship between EDD and conductance. The parameter details of

theoretical calculation and machine learning are shown in Table S1 in the supplementary information.

Conclusion

In this paper, we investigate the modulation of edge-state and bulk-state transport properties in HgTe/CdTe quantum well under piezotronic effect. Piezoelectric potential is created by external strains to adjust the radius of the depletion region, influence the conductance and EDD. The edge-state conductance exhibits an excellent switching behavior. Machine learning is further employed to explore such edge-state transport, and can give much high accuracy for the conductance. This study provides a high-efficient way to search or design high performance quantum piezotronic devices by machine learning.

Reference

1. Wang, Z.L., *Progress in piezotronics and piezo-phototronics.* Advanced Materials, 2012. **24**(34): p. 4632-4646.

2. Wang, Z.L. and J. Song, *Piezoelectric nanogenerators based on zinc oxide nanowire arrays.* Science, 2006. **312**(5771): p. 242-246.

3. Korkusinski, M. and P. Hawrylak, *Quantum strain sensor with a topological insulator HgTe quantum dot.* Scientific reports, 2014. **4**: p. 4903.

4. Zhu, P., et al., *Ultra-high sensitivity strain sensor based on piezotronic bipolar transistor.* Nano energy, 2018. **50**: p. 744-749.

5. Calahorra, Y., et al., *Highly sensitive piezotronic pressure sensors based on undoped GaAs nanowire ensembles.* Journal of Physics D: Applied Physics, 2019.

6. Chen, L., et al., *Strain-gated field effect transistor of a MoS2–ZnO 2D–1D hybrid structure.* ACS nano, 2015. **10**(1): p. 1546-1551.

7. Yu, R., et al., *Piezo-phototronic Boolean Logic and Computation Using Photon and Strain Dual-Gated Nanowire Transistors.* Advanced Materials, 2015. **27**(5): p. 940-947.

8. Kumar, B. and S.-W. Kim, *Energy harvesting based on semiconducting piezoelectric ZnO nanostructures.* Nano Energy, 2012. **1**(3): p. 342-355.

9. Wang, X., et al., *Piezoelectric field effect transistor and nanoforce sensor based on a single ZnO nanowire.* Nano letters, 2006. **6**(12): p. 2768-2772.

10. Zhang, Y., Y. Yang, and Z.L. Wang, *Piezo-phototronics effect on nano/microwire solar cells.* Energy & Environmental Science, 2012. **5**(5): p. 6850-6856.

11. Yang, Q., et al., *Enhancing light emission of ZnO microwire-based diodes by piezo-phototronic effect.* Nano letters, 2011. **11**(9): p. 4012-4017.

12. Liu, Y., et al., *Nanowire Piezo-phototronic Photodetector: Theory and Experimental Design.* Advanced Materials, 2012. **24**(11): p. 1410-1417.

13. Bernevig, B.A., T.L. Hughes, and S.-C. Zhang, *Quantum spin Hall effect and topological phase transition in HgTe quantum wells.* Science, 2006. **314**(5806): p. 1757-1761.

14. König, M., et al., *Quantum spin Hall insulator state in HgTe quantum wells.* Science, 2007. **318**(5851): p. 766-770.

15. Roth, A., et al., *Nonlocal transport in the quantum spin Hall state.* Science, 2009. **325**(5938): p. 294-297.

16. Zhang, L., et al., *Electrical switching of the edge channel transport in HgTe quantum wells with an inverted band structure.* Physical Review B, 2011. **83**(8): p. 081402.

17. Leubner, P., et al., *Strain engineering of the band gap of HgTe quantum wells using superlattice virtual substrates.* Physical review letters, 2016. **117**(8): p. 086403.

18. Liu, Q., et al., *Switching a normal insulator into a topological insulator via electric field with application to phosphorene.* Nano letters, 2015. **15**(2): p. 1222-1228.

19. Guo, X., et al., *Quantum information memory based on reconfigurable topological insulators by piezotronic effect.* Nano Energy, 2019.

20. Dan, M., et al., *High performance piezotronic logic nanodevices based on GaN/InN/GaN topological insulator.* Nano Energy, 2018. **50**: p. 544-551.

21. Miao, M., et al., *Polarization-driven topological insulator transition in a GaN/InN/GaN quantum well.* Physical review letters, 2012. **109**(18): p. 186803.

22. Li, J., et al., *Two-dimensional topological insulators with tunable band gaps: Single-layer HgTe and HgSe.* Scientific reports, 2015. **5**: p. 14115.

23. Krishtopenko, S. and F. Teppe, *Realistic picture of helical edge states in HgTe quantum wells.* Physical Review B, 2018. **97**(16): p. 165408.

24. Brüne, C., et al., *Dirac-screening stabilized surface-state transport in a topological insulator.* Physical Review X, 2014. **4**(4): p. 041045.

25. Olshanetsky, E., et al., *Persistence of a two-dimensional topological insulator state in wide HgTe quantum wells.* Physical review letters, 2015. **114**(12): p. 126802.

26. Pribiag, V.S., et al., *Edge-mode superconductivity in a two-dimensional topological insulator.* Nature nanotechnology, 2015. **10**(7): p. 593.

27. Wu, Z., et al., *Spin-polarized charge trapping cell based on a topological insulator quantum dot.* RSC Advances, 2017. **7**(49): p. 30963-30969.

28. Strunz, J., et al., *Interacting topological edge channels.* Nature Physics, 2020. **16**(1): p. 83-88.

29. Groth, C.W., et al., *Kwant: a software package for quantum transport.* New Journal of Physics, 2014. **16**(6): p. 063065.

30. Saha, S. and J. Kumar, *Fully self-consistent analysis of III-nitride quantum cascade structures.* Journal of Computational Electronics, 2016. **15**(4): p. 1531-1540.

31. Zhang, L.B., et al., *Electrical switching of the edge channel transport in HgTe quantum wells with an inverted band structure.* Physical Review B, 2011. **83**(8): p. 081402.

32. Bernevig, B.A., T.L. Hughes, and S.-C. Zhang, *Quantum Spin Hall Effect and Topological Phase Transition in HgTe Quantum Wells.* Science, 2006. **314**(5806): p. 1757.

33. Landauer, R., *Spatial variation of currents and fields due to localized scatterers in metallic conduction.* IBM Journal of Research and Development, 1957. **1**(3): p. 223-231.

34. Landauer, R., *Electrical transport in open and closed systems.* Zeitschrift für Physik B Condensed Matter, 1987. **68**(2-3): p. 217-228.

35. Rocha, A.R., et al., *Towards molecular spintronics.* Nature Materials, 2005. **4**(4): p. 335-339.

36. Rungger, I. and S. Sanvito, *Algorithm for the construction of self-energies for electronic transport calculations based on singularity elimination and singular value decomposition.* Physical Review B, 2008. **78**(3): p. 035407.

37. Soler, J.M., et al., *The SIESTA method forab initioorder-Nmaterials simulation.* Journal of Physics: Condensed Matter, 2002. **14**(11): p. 2745-2779.

38. Maugin, G.A., *Continuum mechanics of electromagnetic solids*. Vol. 33. 2013: Elsevier.

39. Zhang, Y., Y. Liu, and Z.L. Wang, *Fundamental Theory of Piezotronics.* Advanced Materials, 2011. **23**(27): p. 3004-3013.

40. Ikeda, T., *Fundamentals of piezoelectricity*. 1996: Oxford university press.

41. Bernardini, F., V. Fiorentini, and D. Vanderbilt, *Spontaneous polarization and piezoelectric constants of III-V nitrides.* Physical Review B, 1997. **56**(16): p. R10024.

42. Hu, G., et al., *Piezotronic Transistor Based on Topological Insulators.* ACS Nano, 2018. **12**(1): p. 779-785.

43. Krueckl, V. and K. Richter, *Switching spin and charge between edge states in topological insulator constrictions.* Physical review letters, 2011. **107**(8): p. 086803.

44. Carrasquilla, J. and R.G. Melko, *Machine learning phases of matter.* Nature Physics, 2017. **13**(5): p. 431-434.

45. Li, L., et al., *Machine learning–enabled identification of material phase transitions based on experimental data: Exploring collective dynamics in ferroelectric relaxors.* Science Advances, 2018. **4**(3): p. eaap8672.

46. Rodriguez-Nieva, J.F. and M.S. Scheurer, *Identifying topological order through unsupervised machine learning.* Nature Physics, 2019. **15**(8): p. 790-795.

47. Hermann, J., Z. Schätzle, and F. Noé, *Deep-neural-network solution of the electronic Schrödinger equation.* Nature Chemistry, 2020. **12**(10): p. 891-897.

48. Lian, W., et al., *Machine Learning Topological Phases with a Solid-State Quantum Simulator.* Physical Review Letters, 2019. **122**(21): p. 210503.

49. Orazbayev, B. and R. Fleury, *Far-Field Subwavelength Acoustic Imaging by Deep Learning.* Physical Review X, 2020. **10**(3): p. 031029.

50. Ren, F., et al., *Accelerated discovery of metallic glasses through iteration of machine learning and high-throughput experiments.* Science Advances, 2018. **4**(4): p. eaaq1566.

51. Zhou, Q., et al., *Learning atoms for materials discovery.* Proceedings of the National Academy of Sciences, 2018. **115**(28): p. E6411.

52. Raccuglia, P., et al., *Machine-learning-assisted materials discovery using failed experiments.* Nature, 2016. **533**(7601): p. 73-76.

53. Huang, G., et al. *Densely Connected Convolutional Networks*. in *2017 IEEE Conference on Computer Vision and Pattern Recognition (CVPR)*. 2017.

54. Miao, M.S., et al., *Polarization-Driven Topological Insulator Transition in a GaN/InN/GaN Quantum Well.* Physical Review Letters, 2012. **109**(18): p. 186803.

55. Hu, G. and Y. Zhang, *Quantum piezotronic devices based on ZnO/CdO quantum well topological insulator.* Nano Energy, 2020. **77**: p. 105154.

56. Liu, Z., et al., *Micro-light-emitting diodes with quantum dots in display technology.* Light: Science & Applications, 2020. **9**(1): p. 83.

57. Ouyang, W., et al., *Enhancing the Photoelectric Performance of Photodetectors Based on Metal Oxide Semiconductors by Charge-Carrier Engineering.* Advanced Functional Materials, 2019. **29**(9): p. 1807672.

58. Wu, W. and Z.L. Wang, *Piezotronics and piezo-phototronics for adaptive electronics and optoelectronics.* Nature Reviews Materials, 2016. **1**(7): p. 16031.

Figure captions

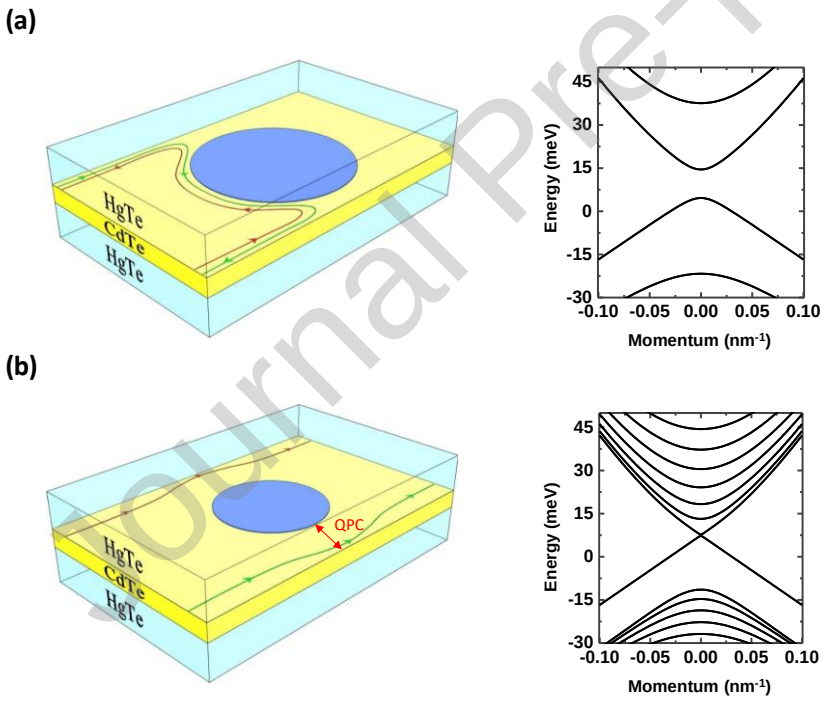

Figure 1. Schematics of electrons transport and band structure in CdTe/HgTe/CdTe quantum well for the radius of circular quantum dot (a) R = 80 nm and (b) R = 20 nm. Spin up (red line) and spin down (green line) electrons travel the circular quantum dot along the opposite boundary.

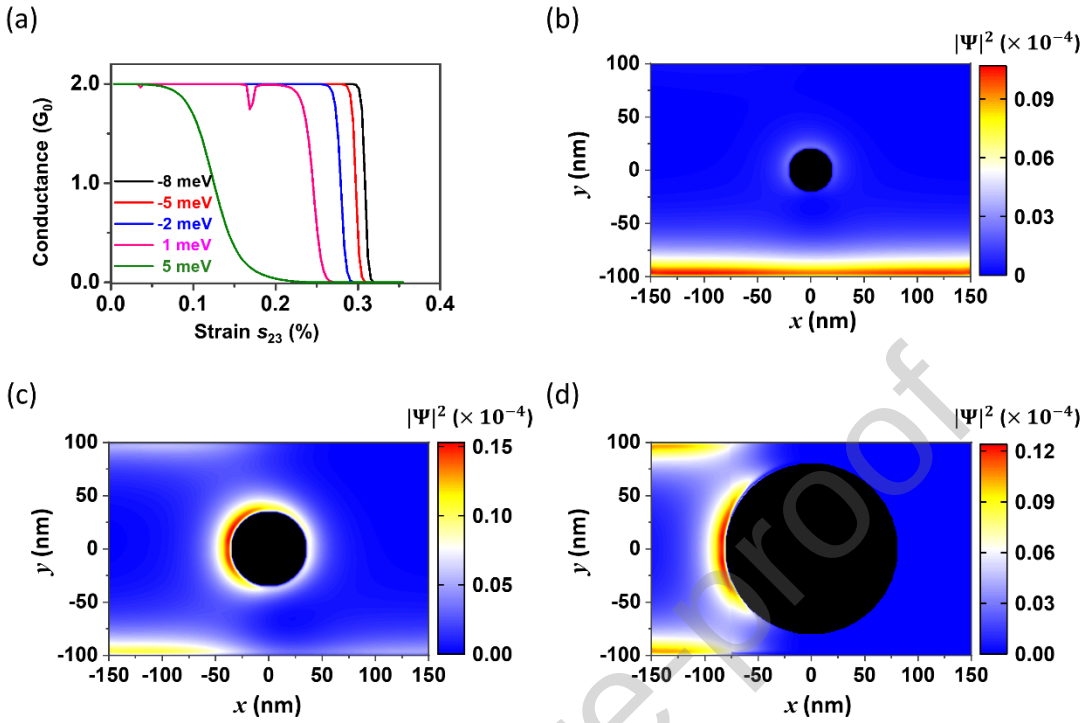

Figure 2. Transport properties of the edge state. (a) The conductance as a function of strain at different Fermi energies uniformly selected in the gapless region. (b) The "ON" state at R = 20 nm (s_{23} = 0.07%) with electrons completely passing along the boundary. (c) The electrons are partially reflected by the quantum point contact at R = 35 nm (s_{23} = 0.13%). (d) The "OFF" state at R = 80 nm (s_{23} = 0.29%) with the electrons completely blocked.

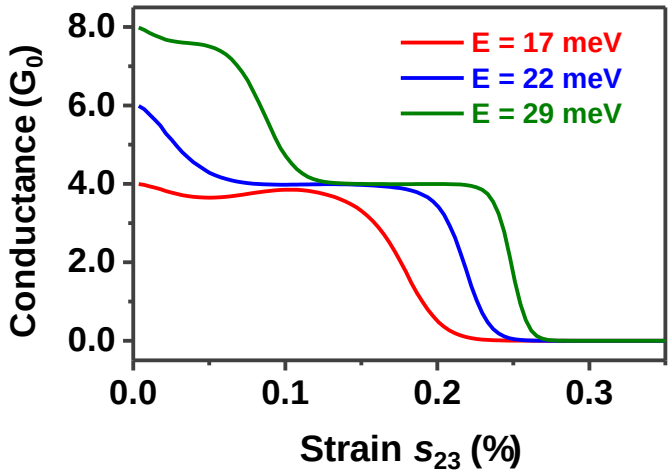

Figure 3. The conductance versus strain under different Fermi energies. These Fermi levels correspond to bulk states.

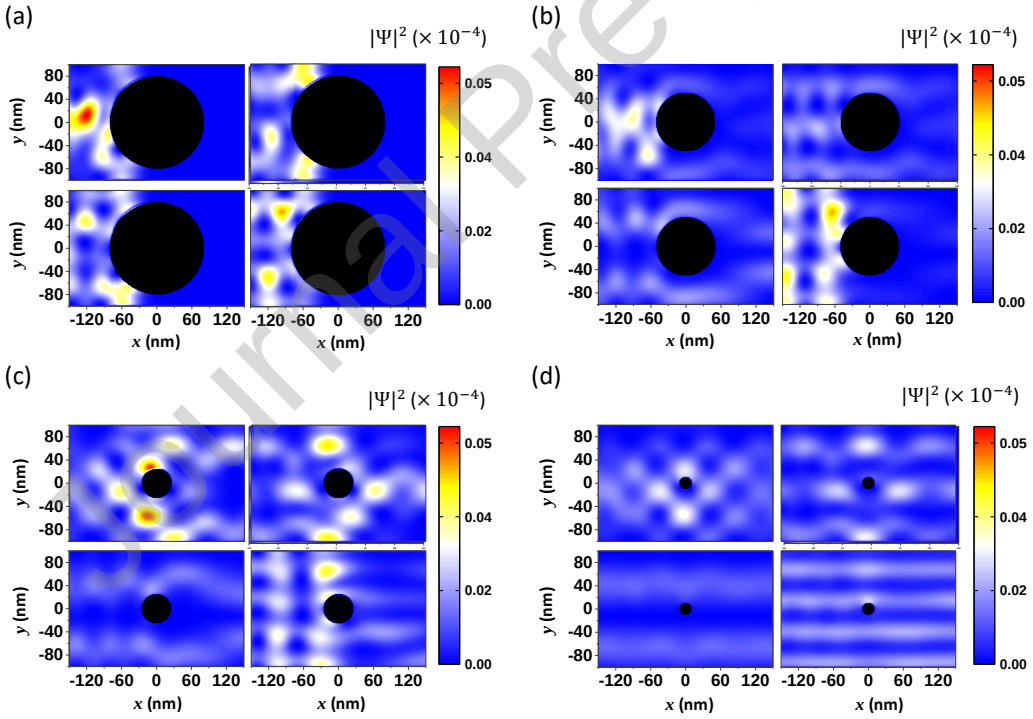

Figure 4. The electronic density distribution at strain (a) s_{23} = 0.29% (R = 80 nm), (b) s_{23} = 0.18% (R = 50 nm), (c) s_{23} = 0.09% (R = 25 nm) and (d) s_{23} = 0.04% (R = 10 nm). Fermi level is fixed at 30 meV with four bulk-state channels.

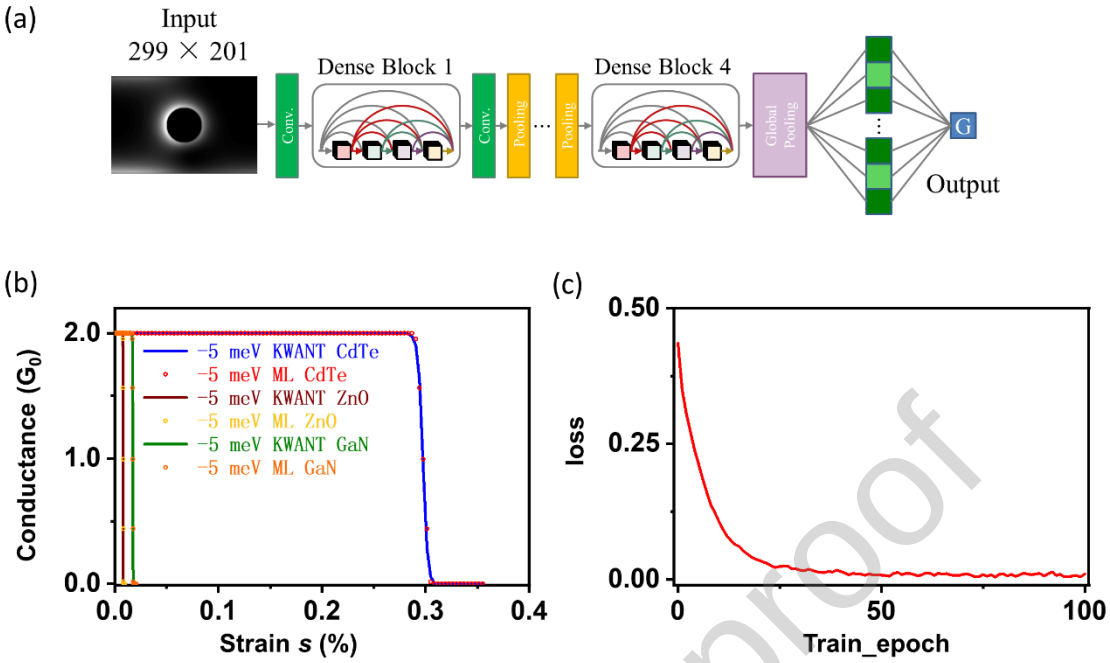

Figure 5. (a) Schematic diagram of machine learning workflow for edge-state transport. The training objects are electronic density distributions and the outputs are conductances. (b) The edge-state conductances of the calculation by KWANT and machine learning predictions of three different materials. (c) DenseNet loss function curve of CdTe material.

Table 1. The machine learning for material science

Description	Calculation method	Result
Deep neural network (DNN) solves electronic Schrödinger equation [47]	DNN	DNN represents electronic wavefunctions to improve computing efficiency
The trained neural networks can identify topological phase [48]	3D convolutional neural networks (CNN)	CNN identifies different topological phases with a success rate of over 90%

DNN recognizes and images subwavelength features from the far-field [49]	DNN	DNN recovers λ/30 details from the far-field with classification accuracy of 80%
ML model and high-throughput (HiTp) experimentation discovers new materials [50]	ML model and HiTp experimentation	The approach discovered three new glass-forming systems
Unsupervised learning to rediscover the periodic table through known existing materials [51]	Neural network	ML learned the basic properties of atoms from known compounds and materials
Machine learning discovers new materials by learning failed experiments information [52]	Support vector machine (SVM)	ML predicted conditions for new materials formation with a success rate of 89%
DenseNet predicted conductance through EDD (Our works)	DenseNet	R-squared is 0.999 of the conductance from the numerical calculation and DenseNet

Graphical Abstract

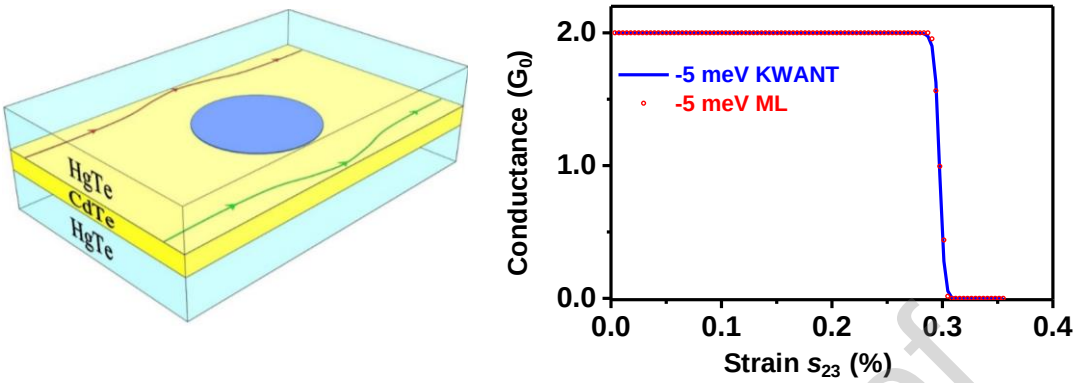

A quantum piezotronic transistor is proposed based on a circular quantum point contact of HgTe/CdTe topological insulator. Edge states and bulk states can be effectively controlled by strain-induced piezoelectric potential. Machine learning is employed to study edge-state transport, which can effectively predict transport conductance.

Highlights

1. Piezotronic effect can effectively control bulk and edge states.
2. The radius of a circular quantum point contact is modulated by strain-induced piezoelectric potential.
3. Machine learning is applied to predict transport conductance of quantum piezotronic devices.

Credit Author Statement

Yuankai Zhou: Methodology, Formal analysis, Writing- Original draft preparation, Validation; **Yuncheng Jiang:** Conceptualization, Methodology, Formal analysis, Writing- Original draft preparation, Validation; **Minjiang Dan:** Conceptualization, Methodology, Formal analysis, Writing- Original draft preparation; **Gongwei Hu:** Conceptualization, Methodology, Formal analysis, Validation; **Lijie Li:** Writing-Reviewing and Editing; **Yan Zhang:** Supervision, Conceptualization, Methodology, Formal analysis, Writing- Reviewing and Editing

Declaration of interests

☒ The authors declare that they have no known competing financial interests or personal relationships that could have appeared to influence the work reported in this paper.

☐The authors declare the following financial interests/personal relationships which may be considered as potential competing interests: